Scientia Iranica B (2013) 20(6), 1709–1719

SCIENTIA IRANICA

Sharif University of Technology
Scientia Iranica
Transactions B: Mechanical Engineering
www.scientiairanica.com

Optimal distribution of braking and steering tire forces subject to stability constraints

A. Tavasoli and M. Naraghi*

Department of Mechanical Engineering, Amirkabir University of Technology, Tehran, P.O. Box 15914, Iran.

Received 19 November 2011; received in revised form 22 May 2013; accepted 15 July 2013

KEYWORDS
Vehicle dynamics;
Adaptive sliding mode control;
Optimal tire force distribution;
Stability constraint.

Abstract. This paper presents an integrated vehicle dynamics control which manages to coordinate steering and braking subsystems using Optimal Distribution of tire Forces (ODF). Specifically, we introduce an ODF scheme, which treats the standard stability conditions of the phase-plane as inequality constraints in the optimization problem. The established scheme works to fulfill the objectives of a higher-level controller, as much as possible, without violating vehicle dynamics stability conditions. A sliding mode enhanced adaptive high-level control assesses the desired total yaw moment and lateral force for vehicle control. The proposed controller only requires online adaptation of control gains without acquiring the knowledge of upper bounds on system uncertainties. An optimization problem incorporating six inequality constraints is solved analytically by Karush-Kuhn-Tucker (KKT) conditions. To coordinate braking and steering subsystems, a phase-plane based adaptation mechanism is suggested to adjust the weighting coefficients in the considered cost function. The simulation cases show that vehicle stability can be improved effectively by the suggested scheme.

1. Introduction

One of the major advances in automotive technology in the past decade has been the development of active safety systems. These systems have recently worked their way into production. Modern passenger cars are now equipped with ABS or/and ESP systems. With the fast emergence of vehicle electronics technologies, utilizing all available actuators (individual tire forces) to improve vehicle dynamics performance has become an active research topic. More recently, optimal distribution of tire forces have been suggested for ground vehicle control systems, in order to use the maximum capacity of tire forces available for control objectives. Optimal tire force distribution to maximize acceleration/deceleration of a four-wheel vehicle during cornering was introduced in [1]. Mokhyamar and Abe [2] presented optimum tire force distribution in order to minimize entire tire workload usage. Wang and Langoria [3] considered a coordinated and reconfigurable vehicle dynamics control system, where the total body forces and moment are distributed between longitudinal slip and slip angle of each tire by a control allocation scheme. Stabilization of vehicles by distributing steering and braking forces through an optimizing dynamic control law was the subject of another study [4]. The notion of adaptive-optimal distribution of tire forces was introduced by the authors in [5]. In another approach [6], an optimizing scheme is suggested to achieve maximum handling with guaranteed vehicle dynamics stability. To distribute vehicle control among individual tire forces constrained under nonlinear saturation conditions, static and dynamic control allocation techniques are introduced into IVDC, [7] and [8], and the results of both methods are compared. Optimized coordination of brakes and

*. *Corresponding author. Tel.: +98 21 64543449*
E-mail addresses: tavasoli@aut.ac.ir (A. Tavasoli); naraghi@aut.ac.ir (M. Naraghi)

active steering for a 4WS passenger car were considered in [9].

In this paper, optimal coordination of steering and braking tire forces constrained to stability conditions is established. The stability condition constraints are derived from the conventional phase-plane approach. The body lateral force and yaw moment for vehicle motion control are determined by a high level sliding mode enhanced adaptive controller. Adaptive control methodology is utilized to update the sliding mode control gains, so that the upper bounds of uncertainties are not required to be known in advance. Then, these forces are fed into a mid-level algorithm to be distributed among the individual steering and braking tire forces. Stability conditions in the phase-plane of the side-slip dynamics are incorporated into the optimal distribution of the tire forces module. In this paper, this is referred to as: "Optimal Distribution of tire Forces Constrained to Stability condition (ODFCS)". Therefore, under normal conditions, where tires have linear characteristics, the ODFCS scheme aims to improve vehicle handling by prioritizing the accomplishment of higher-level control objectives through steering forces, and deactivating the braking subsystem. As the vehicle side-slip motion approaches the boundaries of the stable region, and vehicle dynamics are in the margin of stability, the inequality constraints of the stability conditions are activated by ODFCS to prevent vehicle lateral motion from leaving the stable regime. In this regard, the task of achieving the desired yaw rate is given as much freedom as possible, while retaining the vehicle side-slip dynamics inside the stable region. Under these conditions, the braking subsystem is activated to stabilize the vehicle. For this purpose, a phase-plane based adaptation mechanism is considered to adjust the weighting coefficients of the proposed cost function. The resulting optimization problem consists of four inequalities stemming from braking force constraints and two inequalities of stability condition. Applying the KKT conditions, the inequality optimization problem is solved, analytically, so that the suggested scheme is efficient and suitable for practical implementation, without the use of numeric optimization software. In general, this is an advantage in that implementations on vehicles with low-cost hardware may be considered. Simulation results on a nonlinear vehicle/driver model for various standard test maneuvers under critical conditions of tire forces show that vehicle stability under the presented ODFCS scheme can be enhanced effectively.

2. Sliding mode enhanced adaptive high-level control

In this section, we first design a high-level controller for vehicle handling and stability based on the conventional Sliding Mode Control (SMC). Then, we consider an SMC with an Upper-bounds Adaptation (SMCUA) of uncertainties.

2.1. Conventional sliding mode control

In general, vehicle handling and stability are achieved through the control of yaw rate and side-slip angle, respectively. The desired yaw rate is calculated based on the driver's steering input and vehicle speed. The design procedure is based on a 2DoF vehicle model, where the basic equations are:

$$mV(\dot{\beta} + r) = Y, \tag{1}$$

$$I_z \dot{r} = M, \tag{2}$$

where m and I_z denote the total mass and yaw moment of inertia, from which only the estimates of $\hat{m}$ and $\hat{I}_z$ are available, and V is the vehicle velocity. β and r stand for the actual vehicle side-slip angle and the yaw rate, respectively. M and Y are sum of external moments in the yaw direction and lateral forces acting on the vehicle, respectively. To account for the un-modelled dynamics and uncertainties in modelling actual nonlinear vehicle dynamics, the unknown, but bounded, disturbance terms, ω_β and ω_r, are embedded into each channel to get:

$$mV(\dot{\beta} + r) = Y + \omega_\beta, \tag{3}$$

$$I_z \dot{r} = M + \omega_r. \tag{4}$$

To design the total lateral force (Y) for a zero desired side-slip angle, the sliding surface, s_β, is selected as:

$$s_\beta = \beta. \tag{5}$$

Differentiating this equation and considering Eq. (3):

$$\dot{s}_\beta = \frac{Y}{mV} - r + \frac{\Delta_\beta}{m}, \tag{6}$$

where term $\Delta_\beta = \frac{\omega_\beta}{V}$ is assumed to be bounded by a known value, $\bar{\Delta}_\beta$:

$$|\Delta_\beta| < \bar{\Delta}_\beta. \tag{7}$$

To guarantee the sliding condition;

$$s_\beta \dot{s}_\beta < 0, \tag{8}$$

the desired body lateral force is considered as:

$$Y = V(\hat{m}r + v_\beta), \tag{9}$$

in which $\hat{m}$ is our estimate of m, and v_β is to be designed. Insert Eq. (9) into Eq. (6) to get the left side of Relation (8) as follows:

$$s_\beta \dot{s}_\beta = s_\beta m^{-1}(\Delta_\beta + v_\beta + \tilde{m}r), \tag{10}$$

where the mass estimation error, $\tilde{m} = \hat{m} - m$, is assumed to satisfy:

$$|\tilde{m}| = |\hat{m} - m| < \bar{m}, \qquad \bar{m} > 0, \tag{11}$$

whose combination with Eqs. (10) and (7) results in:

$$\begin{aligned} s_\beta \dot{s}_\beta &\leq m^{-1}(s_\beta v_\beta + |\Delta_\beta||s_\beta| + |\tilde{m}||r||s_\beta|) \\ &< m^{-1}(s_\beta v_\beta + \bar{\Delta}_\beta|s_\beta| + \bar{m}|r||s_\beta|). \end{aligned} \tag{12}$$

To achieve Relation (8), v_β is considered to be:

$$v_\beta = -k_\beta \text{sgn}(s_\beta), \tag{13}$$

where sgn(.) is the signum function, and:

$$k_\beta > \bar{\Delta}_\beta + \bar{m}|r| + \eta_\beta, \qquad \eta_\beta > 0. \tag{14}$$

By substituting Eq. (13) into Eq. (9), the desired body lateral force is attained. To mitigate the problem of chattering, the sign function is replaced by a saturation function with a boundary layer thickness of $\Phi_\beta > 0$. Thus, the final control law becomes:

$$Y = V\left(\hat{m}r - k_\beta \text{sat}\left(s_\beta/\Phi_\beta\right)\right). \tag{15}$$

In order to design the body yaw moment (M) for tracking the desired yaw rate (r_d), the sliding surface, s_r, is adopted as:

$$\begin{aligned} s_r &= (r - r_d) + \lambda_r \int_0^t (r - r_d) d\tau, \\ \lambda_r &> 0, \end{aligned} \tag{16}$$

where the integral term is used to mitigate the undesirable yaw angle offset and ensure the desired vehicle heading. Differentiating Eq. (16) along with Eq. (4) leads to:

$$\begin{aligned} \dot{s}_r &= \frac{M}{I_z} + \frac{\omega_r}{I_z} - \tau, \\ \tau &= \dot{r}_d - \lambda_r(r - r_d). \end{aligned} \tag{17}$$

The design process of the desired body yaw moment is similar to that of Eq. (15):

$$\begin{aligned} M &= \hat{I}_z(\dot{r}_d - \lambda_r(r - r_d)) - k_r \text{sat}\left(\frac{s_r}{\Phi_r}\right), \\ \Phi_r &> 0, \end{aligned} \tag{18}$$

where $\hat{I}_z$ is an estimate of I_z and:

$$\begin{aligned} k_r &> \bar{\Delta}_r + \bar{I}_z|\dot{r}_d - \lambda_r(r - r_d)| + \eta_r, \\ \eta_r &> 0, \end{aligned} \tag{19}$$

with $\bar{\Delta}_r > 0$ and $\bar{I}_z > 0$ being the upper bounds for $|\omega_r|$ and $|\tilde{I}_z| = |\hat{I}_z - I_z|$, respectively.

2.2. Sliding mode enhanced adaptive control

From Relations (14) and (19), it can be observed that selection of SMC gains, k_β and k_r, depends on upper bounds of uncertainties in vehicle dynamics and body mass and inertia, i.e. $\bar{\Delta}_r$, $\bar{\Delta}_\beta$, $\bar{m}$ and $\bar{I}_z$. In practice, uncertainties and disturbances depend primarily on the highly nonlinear dynamics of the vehicle and tires, which are not completely known, and one cannot determine their exact bounds too. So, no universal method is available yet to tune the controller gains, and these gains are tuned by a trial and error approach in practical implementations. In this regard, the controller tends to be over-conservative, which may induce a poor tracking performance, as well as undesirable oscillations in the control signal. To overcome this drawback, the adaptive control methodology, with control parameters updated online, is a promising approach. In this section, we use the adaptive control technique to attain a Sliding Mode Controller with Upper bound Adaptation (SMCUA). To design sliding mode controls with variable gains, the following modified control laws are established:

$$Y = V\left(\hat{m}r - \left(\hat{k}_{\beta 1} + \hat{k}_{\beta 2}|r|\right)\text{sgn}(s_\beta)\right), \tag{20}$$

$$M = \hat{I}_z \tau - \left(\hat{k}_{r1} + \hat{k}_{r2}|\tau|\right)\text{sgn}(s_r), \tag{21}$$

where:

$$\tau = \dot{r}_d - \lambda_r(r - r_d), \tag{22}$$

and the varying controller gains are updated as:

$$\dot{\hat{k}}_{\beta 1} = \gamma_{\beta 1}^{-1}|s_\beta|, \qquad \gamma_{\beta 1} > 0, \tag{23}$$

$$\dot{\hat{k}}_{\beta 2} = \gamma_{\beta 2}^{-1}|r||s_\beta|, \qquad \gamma_{\beta 2} > 0, \tag{24}$$

$$\dot{\hat{k}}_{r1} = \gamma_{r1}^{-1}|s_r|, \qquad \gamma_{r1} > 0, \tag{25}$$

$$\dot{\hat{k}}_{r2} = \gamma_{r2}^{-1}|\tau||s_r|, \qquad \gamma_{r2} > 0. \tag{26}$$

Assume that there are positive constants, $k_{\beta 1}^d$, $k_{\beta 2}^d$, k_{r1}^d and k_{r2}^d, that satisfy:

$$k_{\beta 1}^d > |\Delta_\beta|, \qquad k_{\beta 2}^d > |\tilde{m}|, \tag{27}$$

$$k_{r1}^d > |\Delta_r|, \qquad k_{r2}^d > |\tilde{I}_z|. \tag{28}$$

It should be noted that we need only to assure that such constants exist without acquiring the knowledge of these upper bounds to use in control laws. Also, consider:

$$\tilde{k}_{\beta 1} = \hat{k}_{\beta 1} - k_{\beta 1}^d, \qquad \tilde{k}_{\beta 2} = \hat{k}_{\beta 2} - k_{\beta 2}^d, \tag{29}$$

$$\tilde{k}_{r1} = \hat{k}_{r1} - k_{r1}^d, \qquad \tilde{k}_{r2} = \hat{k}_{r2} - k_{r2}^d. \tag{30}$$

Then, the stability of the considered adaptive-

sliding mode control laws can be shown through Lyapunov candidates:

$$V_\beta = \frac{m}{2}s_\beta^2 + \frac{1}{2}\gamma_{\beta 1}\tilde{k}_{\beta 1}^2 + \frac{1}{2}\gamma_{\beta 2}\tilde{k}_{\beta 2}^2, \quad (31)$$

$$V_r = \frac{I_z}{2}s_r^2 + \frac{1}{2}\gamma_{r1}\tilde{k}_{r1}^2 + \frac{1}{2}\gamma_{r2}\tilde{k}_{r2}^2. \quad (32)$$

To prove the stability of the side-slip angle under Eq. (20) with adaptation laws in Eqs. (23) and (24), first insert Eq. (20) into Eq. (6), so that:

$$m\dot{s}_\beta = \left(\tilde{m}r + \Delta_\beta - \left(\hat{k}_{\beta 1} + \hat{k}_{\beta 2}|r|\right)\mathrm{sgn}(s_\beta)\right). \quad (33)$$

Then, differentiate Eq. (31) and get:

$$\dot{V}_\beta = ms_\beta\dot{s}_\beta + \left(\gamma_{\beta 1}\tilde{k}_{\beta 1}\dot{\tilde{k}}_{\beta 1} + \gamma_{\beta 2}\tilde{k}_{\beta 2}\dot{\tilde{k}}_{\beta 2}\right). \quad (34)$$

Replacing Eq. (33) in Eq. (34) and considering Eq. (29), we have:

$$\begin{aligned}\dot{V}_\beta =& \left(\tilde{m}r + \Delta_\beta - \left(\hat{k}_{\beta 1} + \hat{k}_{\beta 2}|r|\right)\mathrm{sgn}(s_\beta)\right)s_\beta \\ &+ \left(\gamma_{\beta 1}\dot{\hat{k}}_{\beta 1}\hat{k}_{\beta 1} + \gamma_{\beta 2}\dot{\hat{k}}_{\beta 2}\hat{k}_{\beta 2}\right) \\ &- \left(\gamma_{\beta 1}\dot{\hat{k}}_{\beta 1}k_{\beta 1}^d + \gamma_{\beta 2}\dot{\hat{k}}_{\beta 2}k_{\beta 2}^d\right). \end{aligned} \quad (35)$$

Using adaptation laws in Eqs. (23) and (24) in Eq. (35) and considering Relation (27) results in:

$$\begin{aligned}\dot{V}_\beta =& \left(\tilde{m}r + \Delta_\beta\right)s_\beta - k_{\beta 1}^d|s_\beta| - k_{\beta 2}^d|r||s_\beta| \\ \leq& \left(|\tilde{m}||r| + |\Delta_\beta|\right)|s_\beta| - k_{\beta 1}^d|s_\beta| - k_{\beta 2}^d|r||s_\beta| \\ =& \left(|\tilde{m}| - k_{\beta 2}^d\right)|r||s_\beta| + \left(|\Delta_\beta| - k_{\beta 1}^d\right)|s_\beta| < 0, \end{aligned} \quad (36)$$

where we use $s_\beta\mathrm{sgn}(s_\beta) = |s_\beta|$. Accordingly, the convergence of s_β to zero and also the boundedness of $\tilde{k}_{\beta 1}$ and $\tilde{k}_{\beta 2}$ are resulted by Barbalat lemma.

In an identical way, the stability of the yaw motion can be demonstrated, first, by combining Eqs. (17) and (21), so that:

$$I_z\dot{s}_r = \tilde{I}_z\tau + \Delta_r - \left(\hat{k}_{r1} + \hat{k}_{r2}|\tau|\right)\mathrm{sgn}(s_r). \quad (37)$$

Differentiate Eq. (32) and replace Eq. (37) for $I_z\dot{s}_r$ to get:

$$\begin{aligned}\dot{V}_r =& \left(\tilde{I}_z\tau + \Delta_r - \left(\hat{k}_{r1} + \hat{k}_{r2}|\tau|\right)\mathrm{sgn}(s_r)\right)s_r \\ &+ \left(\gamma_{r1}\dot{\hat{k}}_{r1}\hat{k}_{r1} + \gamma_{r2}\dot{\hat{k}}_{r2}\hat{k}_{r2}\right) \\ &- \left(\gamma_{r1}\dot{\hat{k}}_{r1}k_{r1}^d + \gamma_{r2}\dot{\hat{k}}_{r2}k_{r2}^d\right). \end{aligned} \quad (38)$$

Using adaptation laws in Eqs. (25) and (26) as well as the inequalities in Relation (28), we have:

$$\begin{aligned}\dot{V}_r =& \left(\tilde{I}_z\tau + \Delta_r\right)s_r - k_{r1}^d|s_r| - k_{\beta 2}^d|\tau||s_r| \\ \leq& \left(|\tilde{I}_z||\tau| + |\Delta_r|\right)|s_r| - k_{r1}^d|s_r| - k_{r2}^d|\tau||s_r| \\ =& \left(|\tilde{I}_z| - k_{r2}^d\right)|\tau||s_r| + \left(|\Delta_r| - k_{r1}^d\right)|s_r| < 0. \end{aligned} \quad (39)$$

Thus, according to the Barbalat lemma, the system state can be driven to the sliding surface, s_r, and the controller gains, $\tilde{k}_{r1}$ and $\tilde{k}_{r2}$, will be bounded. Furthermore, to tackle the chattering problem, a saturation function is used to derive the final adaptive control laws:

$$Y = V\left(\hat{m}r - \left(\hat{k}_{\beta 1} + \hat{k}_{\beta 2}|r|\right)\mathrm{sat}\left(s_\beta/\Phi_\beta\right)\right), \quad (40)$$

$$M = \hat{I}_z\tau - \left(\hat{k}_{r1} + \hat{k}_{r2}|\tau|\right)\mathrm{sat}\left(\frac{s_r}{\Phi_r}\right). \quad (41)$$

3. Optimal distribution of steering and braking tire forces

With the optimal distribution of tire forces we seek to attain two main goals. One is to utilize the maximum capability of tire forces and the other is to manage the active steering and braking subsystems. These are accomplished by considering and optimizing a convenient, two part cost function. The first step, which is a summation of squared normalized resultant tire forces (tires workload), is to minimize tires workload, and the second, being the squared summation of normalized longitudinal tire forces, enables adjusting the steering and braking contributions in an integrated vehicle dynamics control scheme. The cost function is written as:

$$f(\mathbf{u}) = \sum_{i=1}^{4}\left\{A_i\frac{F_{xi}^2 + F_{yi}^2}{(\mu_i F_{zi})^2} + B_i\left(\frac{F_{xi}}{\mu_i F_{zi}}\right)^2\right\}, \quad (42)$$

where i denotes wheel number, F_{xi} and F_{yi} are individual longitudinal and lateral tire forces, F_{zi} is the vertical load, and μ_i is the tire friction coefficient, all defined in the vehicle body fixed coordinate system, as shown in Figure 1. Also, A_i and B_i are weighting coefficients to be adjusted, and $\mathbf{u} = [F_{x1}, F_{x2}, F_{x3}, F_{x4}, F_{y1}, F_{y2}, F_{y3}, F_{y4}]$ is the control system input. It is assumed that each wheel can be steered/braked independently and also that only braking torque at the wheels is possible.

The weighting coefficient, B_i, is updated by means of an adaptation mechanism to coordinate steering and braking subsystems [5]. The sum of the lateral forces and yaw moments acting on the vehicle by each

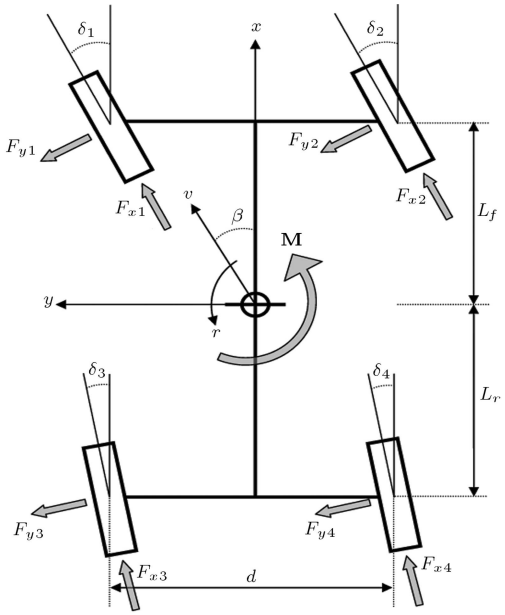

Figure 1. Vehicle dynamics model schematic in top view.

tire force should be equal to the required total lateral force, Y, and yaw moment, M, computed based on the presented higher-level control. Therefore, referring to Figure 1, all variables in the objective function must satisfy the two equality constraints, as follows:

$$Y = \sum_{i=1}^{4} F_{yi}, \tag{43}$$

$$M = \sum_{i=1}^{2} \left(L_f F_{yi} - L_r F_{y(i+2)}\right) + \frac{d}{2} \sum_{i=1}^{2} \left(F_{x(2i)} - F_{x(2i-1)}\right). \tag{44}$$

On the other hand, in this research, it is assumed that the applied torque at each wheel is only the braking torque, and the driveline torque is not possible. These words are written as:

$$C_j(\mathbf{u}) = F_{xj} \leq 0, \qquad j = 1, \cdots, 4. \tag{45}$$

Thus, the cost function contains eight variables, which should satisfy two equality constraints (Eqs. (43) and (44)) and four inequality constraints (Eq. (45)). Then, it is shown that the objective function and the constraint functions are convex, and KKT conditions are used to provide an analytical solution for the constrained optimization problem [5].

4. Construction of the stability constraints

According to vehicle state analysis in the β-$\dot{\beta}$ plane [10], vehicle stability is related directly to the side-slip

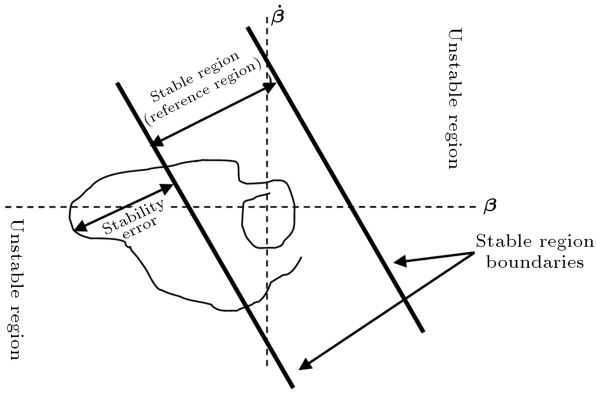

Figure 2. Different regions in β-$\dot{\beta}$ phase-plane.

motion and, hence, stability is accomplished through limiting this motion. A description of the various regions in the phase-plane of side-slip dynamics has been shown in Figure 2 for the reference region of stability control definition. As demonstrated in [10], inside the stable region, the vehicle state is stable and no more active control is needed for vehicle stability. As the vehicle states leaves the stable region, a stability controller is activated to stabilize vehicle motion.

The boundary of the stable region is given by [11]:

$$\left|\frac{1}{24}\dot{\beta} + \frac{4}{24}\beta\right| < 1. \tag{46}$$

As can be seen by Eq. (46), the stability condition is a bound on the vehicle side-slip angle, β, and its time-derivative, $\dot{\beta}$. To be incorporated into the ODF problem as inequality constraints, Eq. (46) has to be transformed into equivalent inequality constraints on control inputs, i.e. individual tire forces. This can be introduced by considering a predicted condition after a time step, T_p.

$$\left|\frac{1}{24}\dot{\beta}^{+} + \frac{1}{24}\beta^{+}\right| < 1, \tag{47}$$

where the superscript "+" refers to the predicted value at the next sampling time. The predicted values can be obtained from Eqs. (1) and (2) of the linear vehicle model. So, by writing the Taylor expansion for β^+ and r^+, preserving only the first order terms, and by considering Eqs. (1) and (2), the predicted values are written as:

$$\beta^{+} = \beta + \dot{\beta}T_p = \beta + \left(\frac{Y}{mV} - r\right)T_p,$$

$$\dot{\beta}^{+} = \frac{F_y^{+}}{mV} - r^{+} = \frac{F_y^{+}}{mV} - (r - \dot{r}T_p) = \frac{F_y^{+}}{mV} - \left(r + \frac{M}{I_z}T_p\right), \tag{48}$$

where F_y^+ is the predicted total lateral force at the

next sampling time. By substituting M and Y from Eqs. (43) and (44) into Eq. (48), and then, the resulted terms into Eq. (47), the stability condition is converted into two linear inequality constraints in terms of control inputs, i.e. individual tire forces. In Eq. (48), F_y^+ is the predicted value for total lateral force at the next sample time and it has not yet been determined at the current instant. Nonetheless, under critical conditions, where the vehicle state approaches the boundaries of the stable region and the lateral tire forces have saturated, the maximum available total lateral force is the product of the tires friction coefficient and the vehicle weight. Here, this value is used as the predicted value for F_y^+, i.e.:

$$F_y^+ = -\mu mg\text{sgn}(\beta). \tag{49}$$

It was seen through a simulation study undertaken under various driving situations that the predicted value of Eq. (49) yields a reasonable assessment for $\dot{\beta}^+$ in Eq. (48), and, hence, for $|\frac{1}{24}\dot{\beta}^+ + \frac{4}{24}\beta^+|$ in Eq. (47), under critical conditions. However, the total available lateral force may be smaller, due to ignoring factors such as the wheels braking effect. Thus, more conservative values can be chosen by considering a fraction of Eq. (49) as:

$$F_y^+ = -c\mu mg\text{sgn}(\beta), \qquad 0 < c < 1. \tag{50}$$

Then, the inequality constraints of stability conditions can be written in the linear form:

$$C_j(\mathbf{u}) = \mathbf{a}_{j-4}^T\mathbf{u} + \mathbf{b}_{j-4} \leq 0, \qquad j = 5, 6, \tag{51}$$

where:

$$\mathbf{a_1^T} = [c_1 \ -c_1 \ c_1 \ -c_1 \ c_2 - c_3 \ c_2 - c_3 \ c_2 + c_4 \ c_2 + c_4],$$

$$\mathbf{a_2} = -\mathbf{a_1},$$

$$b_1 = \frac{1}{24}\left(4\beta - (1 + 4T_p)r - \frac{\mu g\text{sgn}(\beta)}{V}\right) - 1,$$

$$b_2 = -b_1 - 2,$$

$$c_1 = \frac{dT_p}{48I_z}, \qquad c_2 = \frac{T_p}{6mV},$$

$$c_3 = \frac{L_f T_p}{24I_z}, \qquad c_4 = \frac{L_r T_p}{24I_z}. \tag{52}$$

5. Optimal distribution of tire forces subjected to stability constraints

In this section, the inequalities of stability condition in Eq. (51) are incorporated into the described ODF in Section 3. An optimization problem subjected to six inequality constraints is derived and solved analytically by applying KKT conditions. First, by Eqs. (47) and (48), it can be seen that the stability conditions are equivalent to bounds on Y and M. On the other hand, Y and M are computed by the higher-level control through Eqs. (40) and (41), which are treated as equality conditions in ODF. This may induce inconsistencies in which the designed values of Y and M might not satisfy the result of Eqs. (47) and (48). In general, to avoid infeasibilities due to conflict between equality and inequality constraints in an optimization problem, the equality constraints can be embedded in the cost function [12]. Thus, here, the new objective is considered as:

$$\begin{aligned} J(\mathbf{u}) =& \rho \sum_{i=1}^{4} \left\{ A_i \frac{F_{xi}^2 + F_{yi}^2}{(\mu_i F_{zi})^2} + B_i \left(\frac{F_{xi}}{\mu_i {F_{zi}}^2} \right)^2 \right\} \\ &+ \left(F_y - \sum_{i=1}^{4} F_{yi} \right)^2 \\ &+ \left(M - \sum_{i=1}^{2} (L_f F_{yi} - L_r F_{y(i+2)}) \right. \\ &\left. + \frac{d}{2} \sum_{i=1}^{2} (F_{x(2i)} - F_{x(2i-1)}) \right)^2, \end{aligned} \tag{53}$$

in which $\rho > 0$ is used to adjust the relative weighting of different terms. The weighting coefficient, B_i, in Eq. (53), is updated by means of a phase-plane based adaptation mechanism. The values of weighting coefficient B_i determine the contribution of the braking subsystem in the objective function. Thus, when the vehicle states are within a stable region, in order to prevent the negative effects of braking on longitudinal dynamics and disturbances to the driver, coefficient B_i is set to a positive value. Thus, in this region, the contribution of braking in the cost function is increased and, consequently, this subsystem is disabled. As the side-slip dynamics enters the unstable region of the phase-plane, coefficient B_i transits to 0 to decrease the contribution of braking in the cost function. Therefore, in this regime, the braking subsystem is activated to take the advantage of this system for vehicle stabilization. A typical gain adaptation mechanism has been proposed, as shown in Figure 3.

By optimizing Eq. (53) without equality constraints (Eqs. (43) and (44)), the designed values of Y and M in Eqs. (40) and (41) may not be generated exactly, specifically under critical conditions where the vehicle side-slip motion is approaching the boundaries of the stable region and the vehicle is within the margin of stability. However, under such conditions, by minimizing the cost function (Eq. (53)) constrained to the

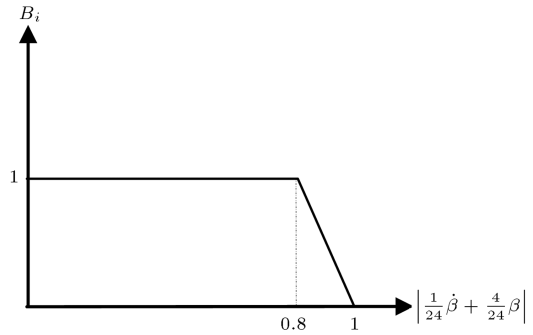

Figure 3. A typical adaptation gain mechanism.

inequalities of the stability conditions (Eq. (47)), the proposed ODFCS works to fulfil the higher-level control objectives (Eqs. (43) and (44)), as much as possible, without violating stability conditions, by maintaining vehicle states inside the stable region. In particular, yaw motion control handling is given as much freedom as possible, provided that the vehicle side-slip motion remains inside the stable regime.The objective function is written in a quadratic form as:

$$J = \frac{1}{2}\mathbf{u}^T\mathbf{G}\mathbf{u} + \mathbf{c}\mathbf{u} + \mathbf{d}, \tag{54}$$

in which:

$$\mathbf{G} = 2(\rho\mathbf{W} + \mathbf{A^T}\mathbf{A}), \qquad \mathbf{c} = -2\mathbf{v^T}\mathbf{A},$$
$$\mathbf{d} = \mathbf{v^T}\mathbf{v}, \tag{55}$$

where $\mathbf{W}$ is the diagonal weighting matrix of F_{xi} and F_{yi} in Eq. (42), when expressed in a quadratic form, and $\mathbf{v}$ is the vector of generalized forces/moment, given by:

$$\mathbf{v} = \begin{bmatrix} Y & M \end{bmatrix}^T, \tag{56}$$

And $\mathbf{A} \in \Re^{2\times 8}$ is a constant matrix, such that:

$$\mathbf{A}\mathbf{u} = \mathbf{v}. \tag{57}$$

Now, the optimization problem is expressed as:

$$\begin{cases} \text{minimize} & J = \frac{1}{2}\mathbf{u^T}\mathbf{G}\mathbf{u} + \mathbf{c}\mathbf{u} + \mathbf{d} \\ \text{subjected to} & \begin{cases} C_j(\mathbf{u}) = F_{xj} \le 0, \\ \qquad j = 1, \cdots, 4 \\ C_j(\mathbf{u}) = \mathbf{a_{j-4}^T}\mathbf{u} + \mathbf{b_{j-4}} \le 0, \\ \qquad j = 5, 6. \end{cases} \end{cases} \tag{58}$$

The problem defined by Eq. (58) is the minimizing of a quadratic cost function constrained to linear inequalities. So, the problem is a convex optimization, and KKT conditions are sufficient and necessary for the problem solution. The KKT condition for Eq. (58) is written as:

$$\frac{\partial J}{\partial u_i} + \sum_{j=1}^{6} \lambda_j \frac{\partial C_j}{\partial u_i} = 0, \qquad i = 1, \cdots, 8,$$
$$\lambda_j C_j = 0, \qquad j = 1, \cdots, 6,$$
$$C_j \le 0, \qquad j = 1, \cdots, 6,$$
$$\lambda_j \ge 0, \qquad j = 1, \cdots, 6, \tag{59}$$

in which λ_j is the Lagrange multiplier corresponding to the jth inequality.

By inspection, it can be demonstrated that from all solutions in Eq. (59), only six cases yield a possible optimal solution, with respect to λ_j and C_j. In each case, $\mathbf{u}$ is obtained as:

$$\mathbf{u} = \mathbf{G^{-1}}[\mathbf{A_I^T}(\mathbf{A_I}\mathbf{G^{-1}}\mathbf{A_I^T})^{-1}(\mathbf{v_I} + \mathbf{A_I}\mathbf{G^{-1}}\mathbf{c^T}) - \mathbf{c^T}], \tag{60}$$

where $\mathbf{A_I}$ and $\mathbf{v_I}$ are derived for λ_j and C_j in each case, as follows:

Case 1:

$$\begin{cases} \lambda_{2,4,5,6} = 0, \\ C_{1,3} = 0 \\ \mathbf{A_I} = [1\ 0\ 0\ 0\ 0\ 0\ 0\ 0; 0\ 0\ 1\ 0\ 0\ 0\ 0\ 0], \\ \mathbf{v_I} = [0; 0]. \end{cases}$$

Case 2:

$$\begin{cases} \lambda_{1,3,5,6} = 0, \\ C_{2,4} = 0 \\ \mathbf{A_I} = [0\ 1\ 0\ 0\ 0\ 0\ 0\ 0; 0\ 0\ 0\ 1\ 0\ 0\ 0\ 0], \\ \mathbf{v_I} = [0; 0]. \end{cases}$$

Case 3:

$$\begin{cases} \lambda_{2,4,6} = 0, \\ C_{1,3,5} = 0 \\ \mathbf{A_I} = [1\ 0\ 0\ 0\ 0\ 0\ 0\ 0; 0\ 0\ 1\ 0\ 0\ 0\ 0\ 0; \mathbf{a}_1^T], \\ \mathbf{v_I} = [0; 0; -b_1]. \end{cases}$$

Case 4:

$$\begin{cases} \lambda_{1,3,6} = 0, \\ C_{2,4,5} = 0 \\ \mathbf{A_I} = [1\ 0\ 0\ 0\ 0\ 0\ 0\ 0; 0\ 0\ 1\ 0\ 0\ 0\ 0\ 0; \mathbf{a}_1^T], \\ \mathbf{v_I} = [0; 0; -b_1]. \end{cases}$$

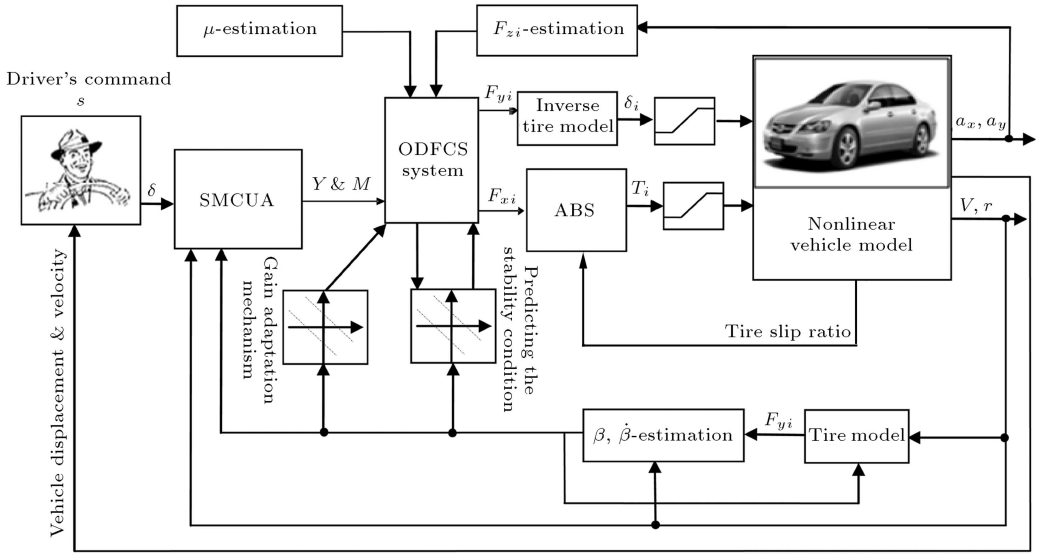

Figure 4. Overall structure of ODFCS applied to integrated vehicle dynamics control.

Case 5:

$$\begin{cases} \lambda_{2,4,5} = 0, \\ \quad C_{1,3,6} = 0 \\ \mathbf{A_I} = [1\ 0\ 0\ 0\ 0\ 0\ 0\ 0; 0\ 0\ 1\ 0\ 0\ 0\ 0\ 0; \mathbf{a}_2^T], \\ \quad \mathbf{v_I} = [0; 0; -b_2]. \end{cases}$$

Case 6:

$$\begin{cases} \lambda_{1,3,5} = 0, \\ \quad C_{2,4,6} = 0 \\ \mathbf{A_I} = [1\ 0\ 0\ 0\ 0\ 0\ 0\ 0; 0\ 0\ 1\ 0\ 0\ 0\ 0\ 0; \mathbf{a}_2^T], \\ \quad \mathbf{v_I} = [0; 0; -b_2]. \end{cases} \quad (61)$$

Then, using the inverse of a simple tire model, the active steering angle of each wheel, δ_i, can be determined, as depicted in [5]. Also, by ignoring the rotational dynamics of wheels, it is assumed that the applied torque at each wheel is equal to the wheel radius times the desired longitudinal force [2]. Moreover, to avoid wheel lock, specifically in critical maneuvers, where the demanded longitudinal forces by optimal distribution of the tire forces module may be high, an ABS for a brake by the wire system is considered to compute the final braking torque, T_i, at each wheel. The overall scheme of the proposed integrated vehicle dynamics control system can be found in Figure 4.

6. Simulation results

Simulations using a 9DOf nonlinear vehicle model have been presented to compare the proposed ODFCS and its performance with that of previous ODF based integrated vehicle dynamics control. Vehicle behavior is examined in the standard single-lane change maneuver. Dugoff's tire model generates tire forces and the vehicle parameters used for simulation are those of a passenger car [13]. Also, a driver model, described and validated experimentally [14], is used to simulate the driver's behavior in maneuvers. The results are, also, compared with those obtained by the proposed method in [5], where no stability constraint is considered in ODF, as described in Section 3 of this paper. The vehicle is assumed to move with an initial velocity of 130 Km/h on a slippery road, where the coefficient of friction is 0.3.

The simulation results for this scenario are depicted in Figures 5-14. As depicted in Figure 5, the vehicle with no active control and only guided by the driver has oscillatory and unstable responses, showing the adverse conditions of the maneuver. Nonetheless, using an active safety control, with either ODF or ODFCS, the vehicle converges onto the intended path of the driver. In addition, as can be seen from Figures 5-7, the vehicle with ODFCS has the best performance in converging to the desired path. Also, it is seen to track the desired yaw rate more properly, and achieve lower side-slip angle, as Figures 8 and 9 reveal. These can be reasoned by referring to the phase-plane trajectories and tire work-load plots in Figures

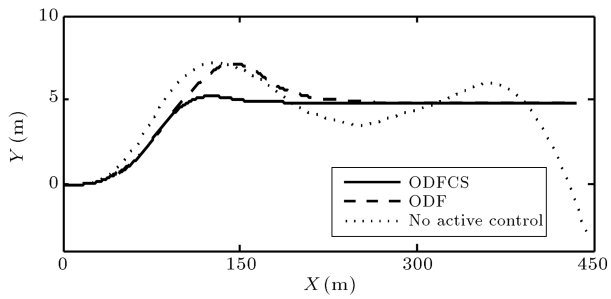

Figure 5. Vehicle path in single lane change manoeuvre.

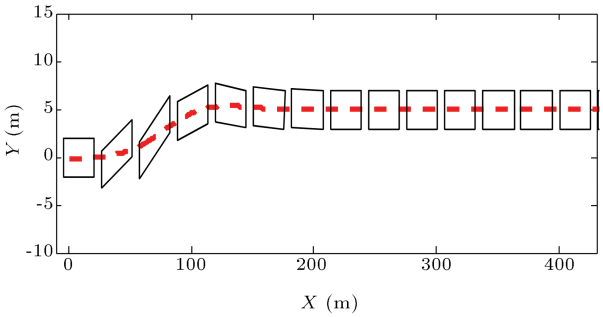

Figure 6. Vehicle path by ODFCS in single lane change manoeuvre.

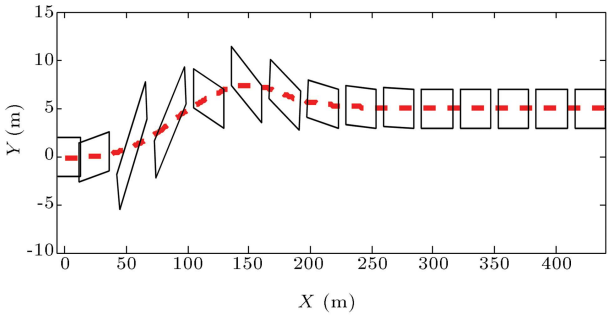

Figure 7. Vehicle path by ODF in single lane change manoeuvre.

10 and 11, respectively. Utilizing the ODFCS system, when the phase-curve approached the stable region boundary, the vehicle state was effectively maintained around this area through proper activation of stability constraints. By bounding the side-slip motion, this approach has also kept the tires away from saturation more efficiently, as depicted in Figure 11. The plot of applied braking torques and active steering are presented in Figures 12 and 13, respectively, to assess how each strategy makes use of the available actuators for vehicle control. As can be seen in Figure 13, active steering by both systems is identical until the vehicle states arrive at the reference boundaries in the phase-plane. Then, the ODFCS method applies counter-steering to stabilize the vehicle, whereas ODF continues

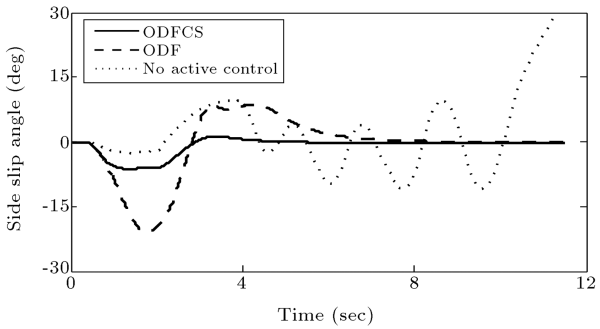

Figure 9. Vehicle side-slip angle in single lane change manoeuvre.

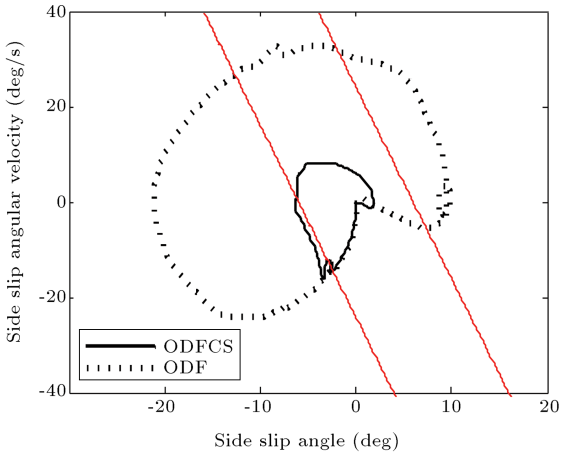

Figure 10. Vehicle state in the phase-plane in single lane change manoeuvre.

to steer the wheels in favor of yaw tracking. Also, active steering by ODFCS is more smooth and proper in comparison with that of ODF. Moreover, Figure 14 shows that the ODF method has induced higher vehicle velocity reduction compared to ODFCS.

7. Conclusion

Optimal distribution of steering and braking tire forces for vehicle stability enhancement was presented in

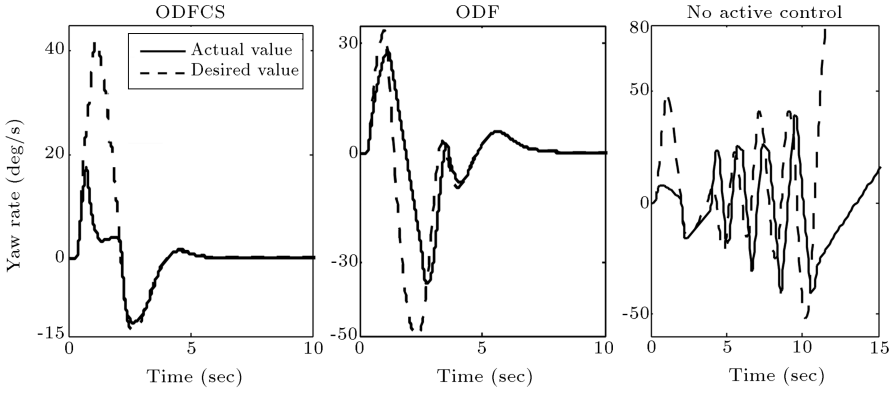

Figure 8. Vehicle side-slip angle in single lane change manoeuvre.

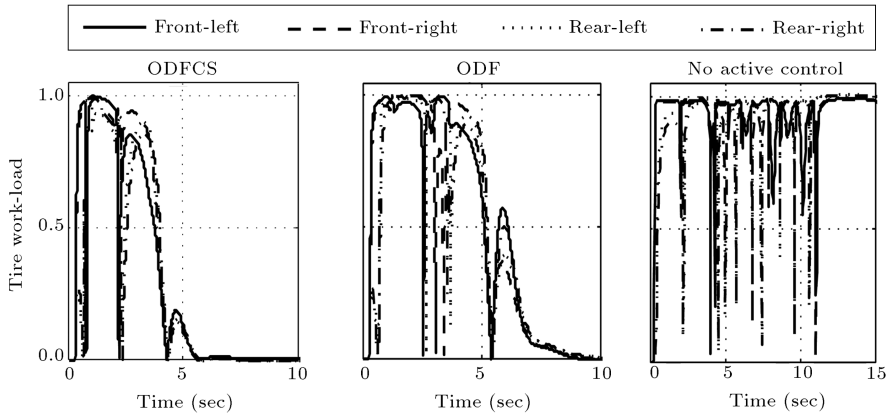

Figure 11. Tires work-load in single lane change manoeuvre.

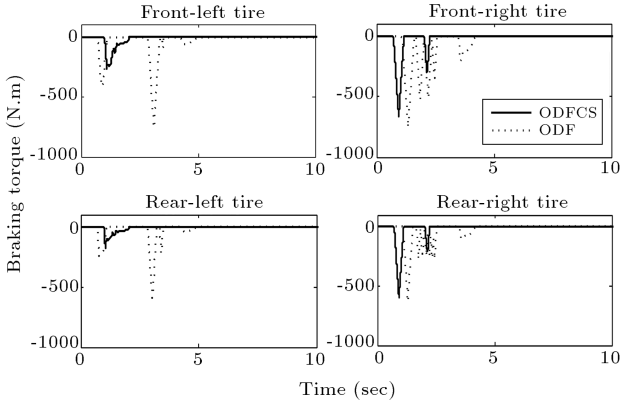

Figure 12. Braking torque applied at wheels in single lane change manoeuvre.

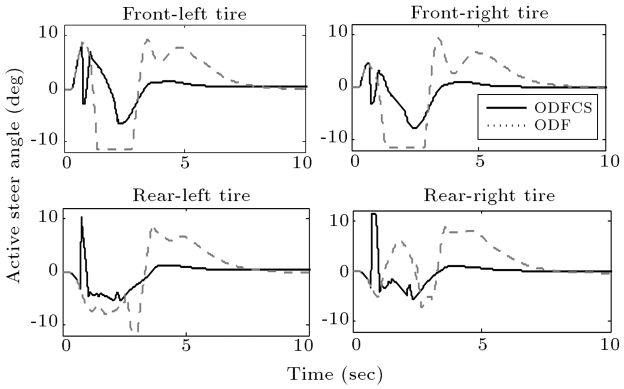

Figure 13. Active steering angle in single lane change manoeuvre.

this paper. The stability condition constraints of a side-slip motion phase-plane may be included in the ODF unit. The total body lateral force and yaw moment were computed through a high-level sliding mode enhanced adaptive controller, where knowledge of the upper bounds of uncertainties is not required. The body forces/moment are distributed among the individul tire forces through the ODFCS module. This induces solving of an optimization problem including

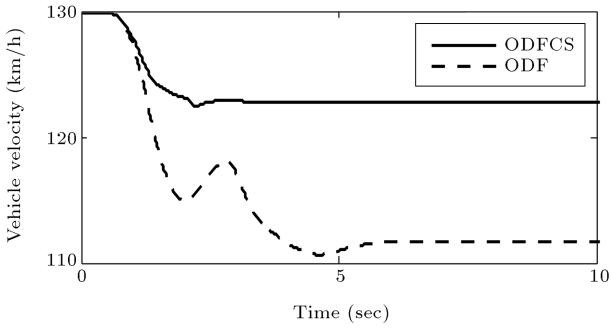

Figure 14. Vehicle longitudinal velocity in single lane change manoeuvre.

six inequality constraints, four inequalty constraints of braking forces and two inequalities of the stability condition, at each instant. An analytical solution was derived for the considered optimization problem, which renders the suggested method more practical for real-time implementation with low-cost hardware. Steering and braking subsystems are coordinated through a phase-plane based gain adaptation mechanism, so that the possible negative effects of the braking subsystem on vehicle longitudinal dynamics are minimized. The effectiveness of the proposed method was evaluted by simulation results.

References

1. Peng, H. and Hu, J.S. "Traction/braking force distribution for optimal longitudinal motion during curve following", *Vehicle System Dynamics*, **26**(4), pp. 301-320 (1999).
2. Mokhyamar, O. and Abe, M. "Simultaneous optimal distribution of lateral tire forces for the model following control", *Journal of Dynamic System, Measurement, and Control*, **126**, pp. 753-763 (2004).
3. Wang, J. and Longoria, R.G. "Coordinated and reconfigurable vehicle dynamics control", *IEEE Transactions on Control Systems Technology*, **17**(3), pp. 723-32 (2009).

4. Tjønnås, J. and Johansen, T.A. "Stabilization of automotive vehicles using active steering and adaptive brake control allocation", *IEEE Transactions on Control Systems Technology*, **18**(3), pp. 545-558 (2010).
5. Naraghi, M., Roshanbin, A. and Tavasoli, A. "Vehicle stability enhancement - an adaptive optimal approach to the distribution of tyre forces", *Proc. IMechE, Part D: J. Automobile Engineering*, **224**, pp. 443-453 (2010).
6. Tavasoli, A. and Naraghi, M. "An optimizing scheme to achieve maximum handling with guaranteed vehicle dynamics stability", *Australian Journal of Science and Technology*, **5**(11), pp. 1989-2001 (2011).
7. Tavasoli, A. and Naraghi, M. "Vehicle sliding mode control with adaptive upper bounds: static versus dynamic allocation to saturated tire forces", *Mathematical Problems in Engineering*, **2012**, pp. 1-31 (2012).
8. Tavasoli, A. and Naraghi, M. "Interior point method to optimize tire force allocation in 4-wheeled vehicles using high-level sliding mode control with adaptive gain", *Asian Journal of Control*, **15**(4), pp. 1-13 (2013).
9. Tavasoli, A., Naraghi, M. and Shakeri, H. "Optimized coordination of brakes and active steering for a 4WS passenger car", *ISA Transactions*, pp. 573-583 (2012).
10. Inagaki, S., Kshiro, I. and Yamamoto, M. "Analysis on vehicle stability in critical cornering using phase-plane method", *Procedings of AVEC'94*, pp. 287-292 (1994).
11. He, J., Crolla, D.A., Levesley, M.C. and Manning, W.J. "Coordination of active steering, driveline, and braking for integrated vehicle dynamics control", *Proc. IMechE, Part D: J. Automobile Engineering*, **220**, pp. 1401-1421 (2006).
12. Nocedal, J. and Wright, S.J., *Numerical Optimization*, 2nd Edn, Springer Science, USA (2006).
13. Rajamani, R., *Vehicle Dynamics and Control*, Springer Science, New York, USA (2006).
14. Abe, M., *Vehicle Handling Dynamics: Theory and Application*, Elsevier Ltd, UK (2009).

Biographies

Ali Tavasoli received his MS and PhD degrees in Mechanical Engineering from Shiraz University, Iran, and Amirkabir University of Technology, Tehran, Iran, in 2006 and 2012, respectively. His research interests include nonlinear control and design techniques for stability and robustness of nonlinear systems, with applications in robotics, vehicles, space systems, and flexible mechanical systems modeled with PDEs.

Mahyar Naraghi received his BS degree from the University of Minnesota, USA, in 1981, his MS degree from Tarbiat Modarres University, Iran, in 1989, and his PhD degree from the University of Ottawa, Canada, in 1996, all in Mechanical Engineering. He is currently with the Department of Mechanical Engineering at Amirkabir University of Technology, Tehran, Iran. His research interests include mobile robots, vehicle dynamics and control, and mechatronics.